Liquid Crystals
Publication details, including instructions for authors and subscription information:
http://www.informaworld.com/smpp/title~content=t713926090

Carborane-containing liquid crystals: a comparison of 4-octyloxy-4-(12-pentyl-1,12-dicarbadodecaboran-1-yl)biphenyl with its hydrocarbon analogues

Krzysztof Czuprynski

To cite this Article Czuprynski, Krzysztof(1999) 'Carborane-containing liquid crystals: a comparison of 4-octyloxy-4-(12-pentyl-1,12-dicarbadodecaboran-1-yl)biphenyl with its hydrocarbon analogues', Liquid Crystals, 26: 2, 261 — 269
To link to this Article: DOI: 10.1080/026782999205407
URL: http://dx.doi.org/10.1080/026782999205407

LIQUID CRYSTALS, 1999, VOL. 26, NO. 2, 261–269

Carborane-containing liquid crystals: a comparison of 4-octyloxy-4′-(12-pentyl-1,12-dicarbadodecaboran-1-yl)biphenyl with its hydrocarbon analogues

KRZYSZTOF CZUPRYNSKI†, ANDREW G. DOUGLASS
and PIOTR KASZYNSKI*
Organic Materials Research Group, Department of Chemistry,
Vanderbilt University, Nashville, TN 37235, USA

and WITOLD DRZEWINSKI
Military University of Technology, Warsaw, Poland

(*Received 9 March 1998; accepted 9 September 1998*)

4-Octyloxy-4′-(12-pentyl-1,12-dicarbadodecaboran-1-yl)biphenyl (**1BC**) has been synthesized along with three hydrocarbon analogues in which the 1,12-dicarbadodecaborane is replaced by a phenyl (**1PH**), *trans*-cyclohexyl (**1CH**) or bicyclo[2.2.2]octyl (**1BO**) ring. The mesogenic properties of these materials have been compared and contrasted in both their pure states and as binary mixtures. The binary phase diagrams for the liquid crystal **1BC**, with its hydrocarbon analogues **1CH** and **1BO** exhibit excellent miscibility of the smectic A phase while the more highly ordered smectic phases (SmB and SmE) for the hydrocarbons are suppressed by **1BC**. In contrast the binary mixture of **1BC** with the terphenyl analog (**1PH**) exhibits complex behaviour in which the thermal stability of the smectic E phase is enhanced. X-ray diffraction data for the **1PH**–**1BC** binary mixture suggest a strong in-plane molecular ordering which might be attributed to intermolecular associations stabilizing the smectic E phase in preference to other smectic modifications.

1. Introduction

We have recently demonstrated that appropriately substituted boron *closo*-clusters exhibit liquid crystallinity [1–6]. The results collected thus far indicate that the cluster-containing mesogens prefer the formation of nematic phases and generally display clearing temperatures somewhat lower than those of the analogous hydrocarbon derivatives. Until now, however, there has been no systematic comparison of the properties of the cluster-containing mesogens and their hydrocarbon analogues, or studies of their intermolecular interactions in mixtures. Such studies are essential for the rational design of new materials and for mixture formulation.

4-Octyloxy-4′-(12-pentyl-1,12-dicarbadodecaboran-1-yl)-biphenyl (**1BC**) [4] (figure 1) exhibits only nematic and monotropic SmA phases. This is in sharp contrast to the mesogenic behaviour of the known terphenyl analogue (**1PH**) which exhibits enantiotropic smectic polymorphism and no nematic phase [7]. This prompted us to study systematically the relationship between these two compounds in both their pure states and as binary mixtures. For further comparison we have also synthesized the analogues with a single bicyclo[2.2.2]octane (**1BO**) or

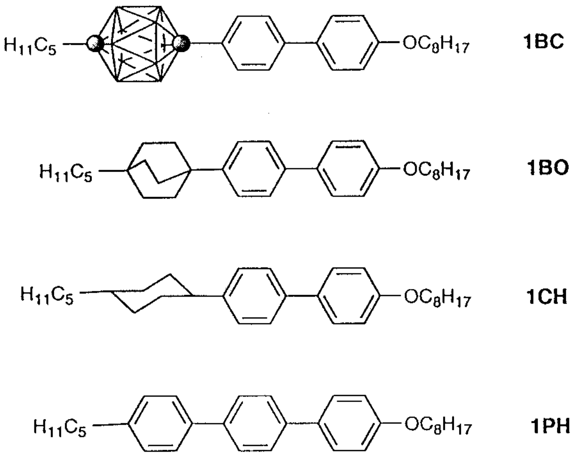

Figure 1. Structures of **1BC**, **1BO**, **1CH** and **1PH**. The carborane representation (**BC1**) has a carbon atom at each position marked with a filled circle and a B–H fragment at every other vertex.

---

*Author for correspondence.

‡The 1997 COBASE fellow on leave from Military University of Technology, Warsaw, Poland.

Journal of Liquid Crystals ISSN 0267-8292 print/ISSN 1366-5855 online ©1999 Taylor & Francis Ltd
http://www.tandf.co.uk/JNLS/lct.htm
http://www.taylorandfrancis.com/JNLS/lct.htm

cyclohexyl (**1CH**) ring (figure 1) and formulated the binary mixtures of each with carborane **1BC**. We augment our studies with computer modelling of the four mesogens and X-ray powder diffraction of two SmE phases.

2. Results

2.1. *Synthesis*

The four mesogenic materials were prepared in coupling reactions of the corresponding two-ring aryl halide **2** and an appropriate organometallic 4-octyloxyphenyl derivative **3** or **4** (see the scheme). Thus **1BC** was prepared from bromide **2BC** [8] and boronic ester **3** [7] under standard Suzuki conditions [9] in 50% yield. The **1CH**, **1PH**, and **1BO** mesogens were prepared from iodides **2CH** [10], **2PH** [11] and **2BO** [10], respectively, and 4-octyloxyphenylmagnesium bromide (**4**) in the presence of NiBr2 according to the general procedure [12].

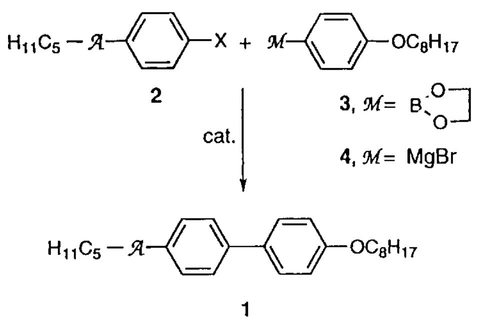

Scheme.

2.2. *Thermal properties*

Temperatures and enthalpies of phase transitions are collected in table 1. The **1PH** and **1CH** derivatives exhibit SmE, SmB, and SmA phases; only the SmE phase for **1CH** is monotropic. Substituting with a bicyclo[2.2.2]octane ring in **1BO** removes the highly organized SmE phase and injects a narrow range nematic. In the carborane derivative both highly ordered smectic phases disappear and the nematic phase range is greatly expanded. The SmA phase is destabilized and is monotropic at 45°C. The stability order for clearing points in this series is **1PH** ~ **1BO** > **1CH** > **1BC** and is in accord with the previously established stability order for similar three-ring systems [13]. The relatively low clearing temperature and the highly expanded nematic phase range in the carborane derivative **1BC**, when compared with the hydrocarbon analogues, parallels our previous observations for other carborane and borane mesogens [1, 2, 4].

The total enthalpy of transition from the crystal to isotropic phase is lowest for the **1BC** and **1BO** derivatives (about 6.3 kcal mol^{-1}). The corresponding enthalpies for the **1PH** and **1CH** are higher by about 2 and 4.5 kcal mol^{-1}, respectively. The DSC analysis suggests a second or pseudo-second order smectic A–nematic transition for **1BC** which is expected for mesogens having wide range nematic phases [14].

The existence of the SmE phase in the terphenyl derivative **1PH** was not reported previously [7]. In the first heating cycle **1PH** exhibits four endotherms as shown in figure 2. Upon cooling only partial crystallization occurs below 20°C and the three remaining transitions

Table 1. Transition temperatures/°C and enthalpies/kcal mol^{-1} for compounds **1**.

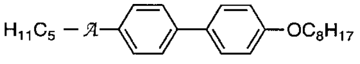

Compound	–𝒜–	Cr		SmE		SmB		SmA		N		I
1PH[a]		•	96.7 3.0	•	194 1.2	•	210.5 1.6	•	221.5 2.7			•
1CH	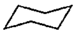	•	56.0 7.4	(•	27.5) 0.4	•	168.5 1.1	•	185.0 1.7			•
1BO		•	89.2 3.9			•	189.9 0.8	•	216.4	•	217.0 1.6[b]	•
1BC	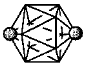	[c] •	71.2 4.8					(•	45.0)[d] [e]	•	148.6 0.3	•

---

[a] Gray, G. W., Hird, M., and Toyne, K. 1991, *Mol. Cryst. Liq. Cryst.*, **195,** 221: Cr 194.5 SmB 221.5 I.

[b] Enthalpy for two transitions (SmA–N and N–I).

[c] Crystal–crystal transition at 65.0°C (1.3 kcal mol^{-1}) is observed.

[d] Measured by optical microscopy.

[e] Second or psuedo-second order transition.

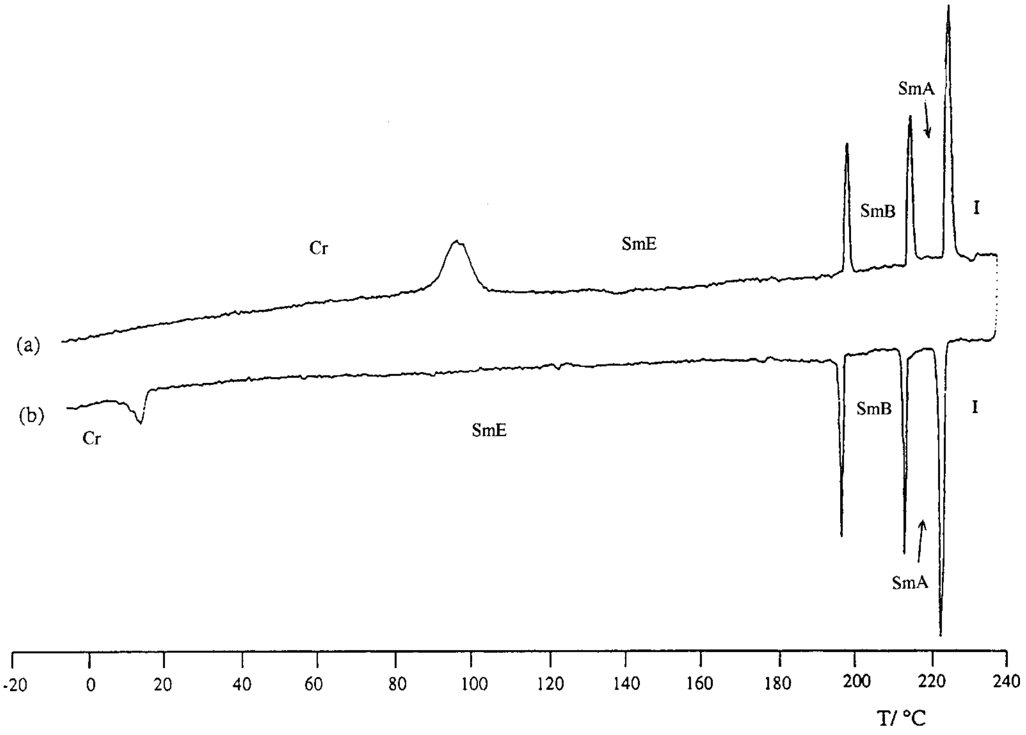

Figure 2. Phase transitions for **1PH** as measured by DSC (*a*) on first heating and (*b*) on first cooling at a scanning rate of 10°C min^{-1}.

show no hysteresis. Thus, the transition at 194.5°C previously identified as melting is ascribed to a smectic E–smectic B transition while the melting process is represented by the first endotherm at 96.7°C. The phase has been identified as SmE based on optical texture, excellent miscibility with other SmE phases (*vide infra*) and enthalpy expected for the SmE–SmB transition [15]. The phase assignment is also supported by evidence from X-ray diffraction studies (*vide infra*).

2.3. *Molecular modelling*

Molecular geometries of the mesogens were fully optimized using the AM1 method and are shown in figure 3. The dimensions of the flexible tails, measured from the first atom of the substituent (oxygen for octyloxy and carbon for pentyl) to the terminal hydrogen atom, are practically constant in the series. The lengths for the OC_8H_{17} and C_5H_{11} tails are 10.78 and 5.93 Å, respectively; the diameter of cylinder of rotation carved by the hydrogen atoms is 2.84 Å for both substituents. The values are given in table 2 and do not include the 1.2 Å van der Waals radius for hydrogen [16]. The octyloxy residue is coplanar with the benzene ring in all four compounds and it forms an angle (defined as terminal carbon atom, oxygen, and C4 of the benzene ring) of 158° with the long molecular axis of the rigid core. The benzene rings in the biphenyl portion of the rigid core form a dihedral angle of 40° which varies little in the series under consideration.

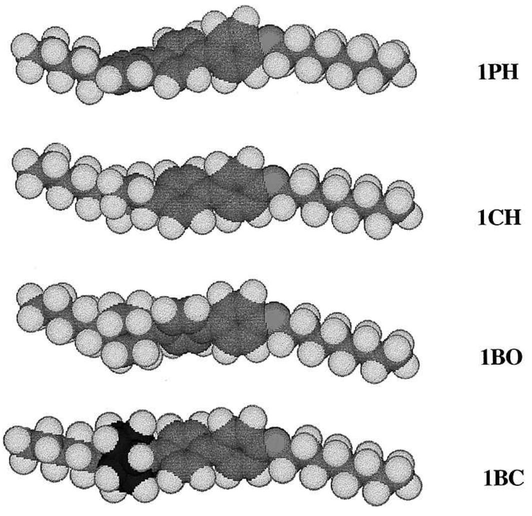

Figure 3. Optimized geometries (AM1) for **1PH**, **1CH**, **1BO** and **1BC**.

The total length of the core (l) measured from CH_2 to O, a diameter of the hydrogen cylinder of rotation for the core (d), the angle of the C_5H_{11} group to the long core axis (α) and the angle between the C_5H_{11} and

Table 2. Calculated (AM1) molecular dimensions for compounds **1**.[a]

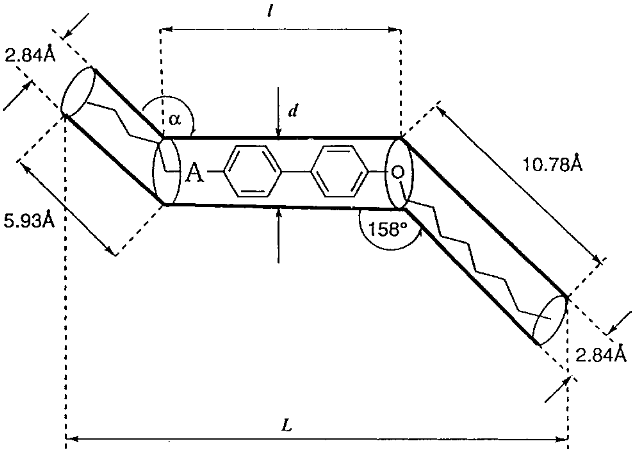

Compound	Core length l	Core width d	C_5H_{11} angle α	Total length[b] L	Inter-chain angle ψ
1PH	14.22	4.3	112.0°	28.00	26.0°
1CH	14.15	4.3	123.0°	29.14	5.0°
1BO	14.09	4.3	116.5°	28.33	12.6°
1BC	14.74	5.0	117.5°	29.14	38.0°

[a] Distances are in Å and angles in degrees.

[b] This value includes a projection of two van der Waals radii of the terminal hydrogen atoms.

C_8H_{17} planes (Ψ) for the four mesogens are shown in table 2.

2.4. *Phase diagrams*

The greatest similarity in the phase behaviour in the considered series is observed for the terphenyl (**1PH**) and cyclohexane (**1CH**) derivatives (table 1). This is supported by an isobaric phase diagram shown in figure 4(*a*) in which all phase transition temperatures change linearly with concentration.

Strong smectogenic character of the **1PH** and **1CH** compounds is evident from their binary phase diagrams with the bicyclo[2.2.2]octane mesogen **1BO** shown in figures 4(*b*) and 4(*c*). The short range nematic phase observed in **1BO** is quickly destabilized by addition of a small mol % of **1PH** or **1CH**, and only SmA–I transitions are observed in mixtures containing less than 95 mol % of **1BO**. Temperatures for the SmA–I and SmB–SmA transitions change linearly with concentration in both diagrams, however, a small minimum in the SmB–SmA line is found at 70 mol % of **1BO**. The SmE phase in the **1PH** and **1CH** derivatives is strongly destabilized by addition of **1BO**.

Binary phase diagrams for the carborane derivative **1BC** with the three hydrocarbon analogues **1BO**, **1CH**, and **1PH** are shown in figures 4(*d–f*), respectively. The N–I and SmA–N transition temperatures in the **1BC–1BO** [figure 4(*d*)] and **1BC–1CH** [figure 4(*e*)] systems change linearly with respect to composition of the mixture. In figure 4(*d*) the SmB–SmA transition temperatures for **1BC–1BO** vary monotonously with concentration until the point of 40 mol % of **1BC**, below which the destabilization of the SmB phase is accelerated so that for 60 mol % of **1BC** only SmA is observed at 0°C.

The **1BC–1CH** binary mixture shows similar behaviour, figure 4(*e*). The phase transition temperatures for SmB–SmA, SmA–N and SmA–I decrease monotonously with the increase of the concentration of **1BC** in the mixture. The temperatures of the N–I transition increase with the decreasing content of **1BC** in the mixture and are 12°C higher than that of pure **1BC** at 80 mol % of **1CH**.

The **1BC–1PH** phase diagram is atypical in the considered series, figure 4(*f*). The SmA–I and SmB–SmA transition temperatures significantly decrease with increasing concentration of **1BC** in **1PH**. The SmB phase forms only in the range of up to 25 mol % of **1BC**, while the SmA phase is discontinuous and exists in two concentration ranges, one below 45 mol % and the other above 80 mol % of **1BC**; these regions are separated by an SmE phase. The SmE–SmB and subsequent SmE–SmA transition temperatures remain virtually unchanged with increasing concentration of **1BC** until 45 mol %, when a SmE–I transition is observed. Further increases in the ratio of **1BC** to **1PH** result in the

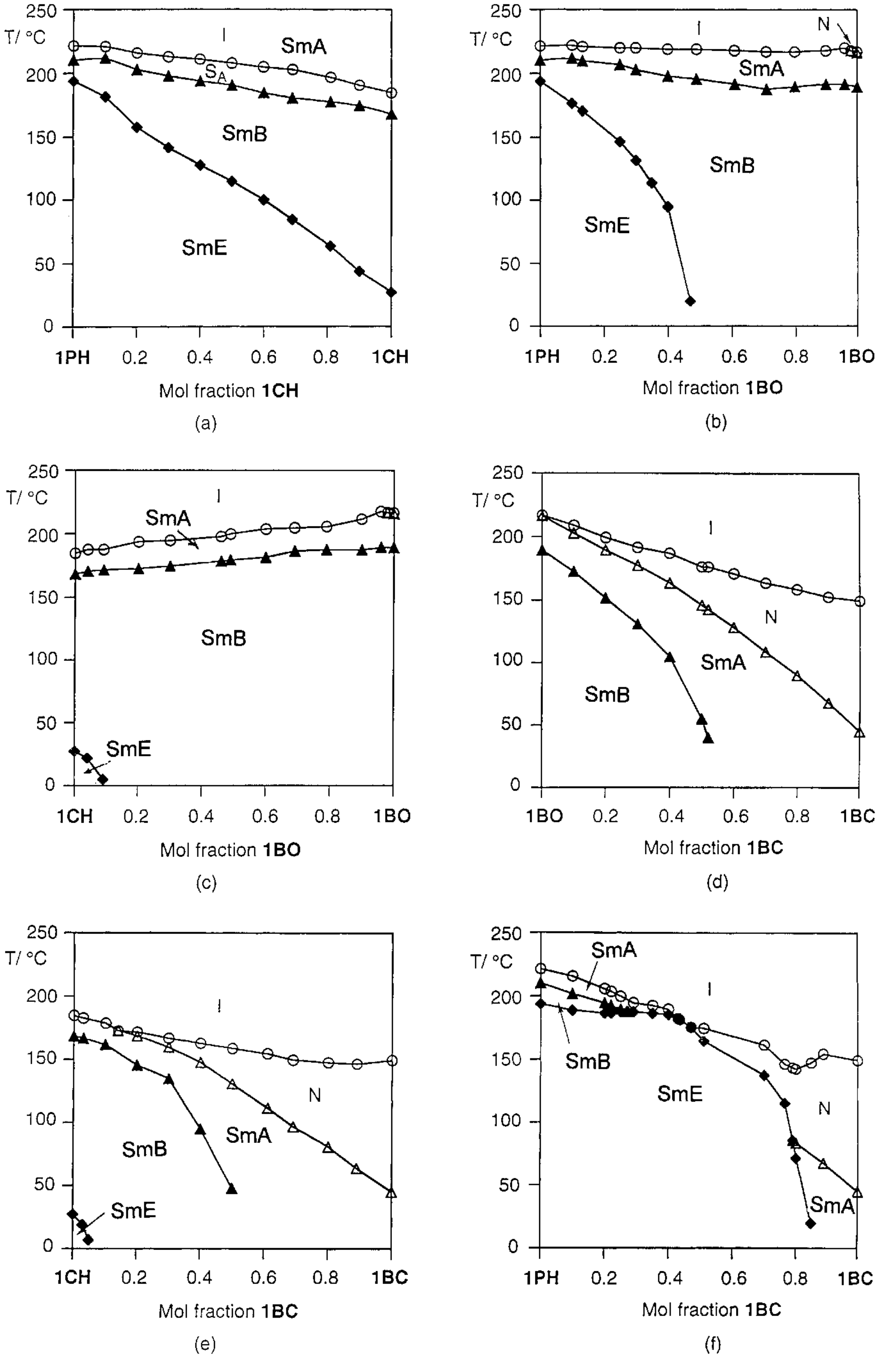

Figure 4. Binary phase diagrams for (*a*) **1PH–1CH**, (*b*) **1PH–1BO**, (*c*) **1CH–1BO**, (*d*) **1BO–1BC**, (*e*) **1CH–1BC** and (*f*) **1PH–1BC**. The lines are guides to the eye.

formation of the nematic as the high temperature mesophase and a concomitant decrease in SmE–N transition temperatures.

The high **1BC** concentration side of the diagram is more unusual. An addition of 10 mol % of **1PH** to pure **1BC** effects increases in both clearing and SmA–N transition temperatures. A further increase in the **1PH** concentration leads to a significant decrease in clearing point which exhibits a minimum at a 4 : 1 ratio of **1BC** to **1PH**. It is at this point that the SmE phase replaces the SmA phase; continuing stabilization of the SmE phase with increasing concentration of **1PH** leads to eradication of nematic behaviour at equimolar composition.

2.5. *X-ray powder diffraction*

The SmE phases identified by microscopy for **1PH** and for its mixture with **1BC** were investigated by X-ray diffraction using samples that had been supercooled to room temperature. The diffraction patterns for these two samples were then compared with that obtained for a

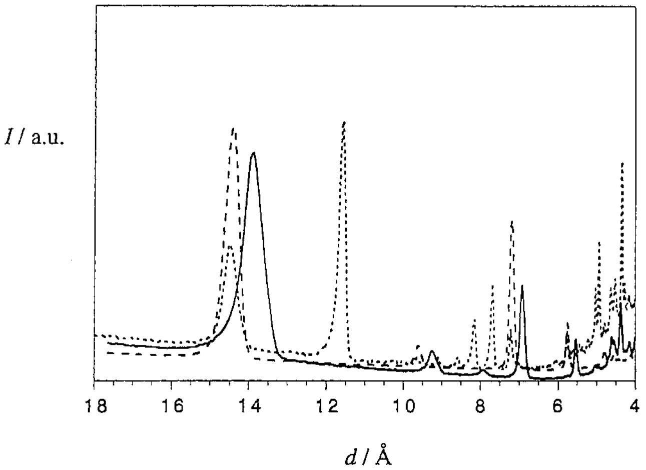

Figure 5. Plot of diffraction intensity (I) as a function of lattice spacing (d) for the **1PH** crystal phase (—), **1PH** supercooled smectic E phase (---), and **1PH–1BC** (57% **1BC**, ---) supercooled smectic E phase.

crystalline sample of **1PH**. These diffraction patterns are shown in figure 5 and the unit cell dimensions and selected reflections are collected in table 3.

3. Discussion

The microscopic and thermal analysis of **1PH–1CH**, **1PH–1BO**, and **1CH–1BO** binary mixtures indicate an ideal miscibility of all phases, figures 4 (*a–c*). The observed destabilization of the SmE phase of **1PH** is in accord with general observations [17, 18] of cases where only one component of a mixture exhibits a particular phase. The destabilization of the nematic phase for **1BO** can be related to its very short temperature range in the pure compound and a strong smectogenic character of the other mixture components (either **1PH** or **1CH**).

The miscibility and the phase behaviour of the carborane-containing compound **1BC** is quite different. While the transition temperatures in phase diagrams for **1BC–1BO** and **1BC–1CH** are in accord with expectations [figures 4 (*d*) and 4 (*e*)], the mixture **1BC–1PH** shows an unexpected expansion of the SmE phase at the expense of the SmA phase, figure 4 (*f*). A similar expansion of the smectic phases, typically accompanied by the appearance of the re-entrant nematic, has been observed in mixtures of polar compounds in which at least one component is an A_d smectogen [19, 20]. Such effects have been attributed to the different layer spacings of smectic A_1 (monolayer) and smectic A_d (partial bilayer) phases. Induction of smectic phases has also been observed in mixtures of compounds in which one constituent possesses a highly polar terminal substituent and the other only non-polar terminal substituents [21–23].

In the case of the **1BC–1PH** binary system [figure 4 (*f*)] both compounds have low polarities and similar molecular dimensions (table 2). The introduction of 20 mol % of **1PH** to **1BC** results in a significant decrease of the clearing point and the appearance of a minimum on the N–I transition curve. This may result from an increase in the long range repulsive dispersion forces which are lowest for the parallel molecular alignment [24]. Presumably the small differences in molecular shapes and dimensions between **1PH** and **1BC** should not result in such a strong effect in the phase stability, especially when the other binary mixtures of **1BC** [figure 4 (*d*) and 4 (*e*)] show no such effect. Nevertheless, the existence of the minimum might be attributed to the formation of **1PH ··· 1BC** molecular associates which are geometrically different from individual molecules of **1BC** forming the nematic phase.

Mixtures of **1BC** with **1CH** or **1BO** show no unusual depression of the nematic phase which suggest that the molecules prefer the ‘head-to-head’ alignment thereby avoiding interactions of the carborane and benzene rings. Lowering the temperature of the **1BC–1PH** mixture (1 : 4) results in weakening of the repulsive dispersive

Table 3. Calculated unit cell dimensions (*abc*), observed (*d*(O)) and calculated (*d*(C)) lattice spacings (in Å) for **1PH** and **1PH–1BC**.

1PH Crystal phase			**1PH** Smectic E phase			**1PH–1BC** Smectic E phase		
$a = 12.01$	$b = 16.59$	$c = 27.78$	$a = 19.19$	$b = 14.85$	$c = 28.86$	$a = 23.13$	$b = 21.89$	$c = 29.04$
h k l	*d*(C)	*d*(O)	*h k l*	*d*(C)	*d*(O)	*h k l*	*d*(C)	*d*(O)
0 0 1	27.775	*	0 0 1	28.859	*	0 0 1	29.037	*
0 0 2	13.888	13.888	0 0 2	14.430	14.430	0 0 2	14.518	14.518
0 0 3	9.258	9.262	2 0 0	9.594	9.623	2 0 0	11.567	11.567
0 2 1	7.949	7.949	0 2 1	7.191	7.191	0 2 1	10.243	10.243
0 0 4	6.944	6.932	3 1 1	5.756	5.756	2 0 2	9.047	9.095
2 1 1	5.535	5.535	4 0 0	4.797	4.787	1 2 2	8.176	8.157
0 2 5	4.616	4.616				2 2 1	7.668	7.689
2 0 4	4.543	4.544				0 2 3	7.251	7.225
2 1 4	4.382	4.371				2 4 0	4.947	4.930

* outside the measurement range.

forces, and attractive interactions between **1BC** and **1PH** molecules become dominant. This results in hindered molecular rotation along the long molecular axis and the formation of the SmE phase. Such intermolecular attractive interactions are much weaker in the mixtures with **1CH** and the SmE phase is destabilized for mixtures of **1BC**–**1CH**.

X-ray powder diffraction data for supercooled smectic phases of pure **1PH** and **1PH**–**1BC** (57 mol% **1BC**) could be indexed only with orthorhombic unit cells. The cell dimensions (table 3) indicate that the thickness of the SmE layers in **1PH** and in the mixture are very similar (28.86 and 29.04 Å, respectively) and correspond to the calculated molecular lengths which are 28.00 and 29.14 Å for **1PH** and **1BC**, respectively (table 2). The introduction of **1BC** to **1PH** results in a significant change in the in-plane unit cell dimensions, $b = 14.85$ Å for the **1PH** smectic E phase and $b = 21.89$ Å for the **1PH**–**1BC** smectic E phase. The 2 0 0 reflection for the **1PH**–**1BC** smectic E phase is actually the most intense while the 2 0 0 reflection for the **1PH** smectic E phase is relatively weak (cf. the 0 0 2 reflection). This indicates that the in-plane ordering is greater in the binary mixture than in the pure **1PH** and these enhanced in-layer intermolecular associations in the binary mixture may serve to stabilize the smectic E phase in preference to other smectic modifications.

4. Conclusions

The binary phase diagrams for the liquid crystal **1BC** with its hydrocarbon analogues **1CH** and **1BO** exhibit excellent miscibility of the smectic A phase. The more highly ordered smectic phases for the hydrocarbons are suppressed by **1BC**. In contrast the binary mixture of **1BC** with the terphenyl analogue **1PH** exhibits complex behaviour in which the smectic E phase is strongly enhanced to the point of being the only liquid crystal phase observed for a narrow range of concentrations. X-ray diffraction data for the **1PH**–**1BC** binary mixture suggest a strong in-plane molecular ordering which might be attributed to intermolecular associations stabilizing the smectic E phase in preference to other smectic modifications.

5. Experimental

5.1. *Characterization*

The phase transition points of the compounds and their mixtures were determined using a PZO 'Biolar' polarizing microscope equipped with a HCS250 Instec hot stage. Thermal analysis was performed using a Mettler DSC 30 instrument. Transition temperatures were obtained using small samples (1–2 mg) and a heating rate of 1°C min^{-1}. In measuring transitional enthalpies, large samples (10–15 mg) and fast heating (10°C min^{-1}) were used. Homogenous mixtures were prepared by evaporation of the CH_2Cl_2 solutions. The phase diagrams were determined by the single concentration method. Full geometry optimizations were performed using the Gaussian 94 [25] computational package and Cerius^2 graphic interface on an SGI workstation. ^{1}H, ^{13}C and ^{11}B NMR spectra were obtained in $CDCl_3$ on Bruker instruments operating at 300 MHz, 75.4 MHz and 64.2 MHz respectively and referenced to the solvent (^{1}H and ^{13}C) or to $B(OMe)_3$. IR spectra were recorded on a Mattson FTIR instrument using thin films of sample deposited on NaCl disks. Mass spectrometry was performed using a Hewlett-Packard 5890 instrument (GCMS). Elemental analysis was provided by Atlantic Microlab, Norcross, Georgia.

X-ray analysis of unoriented samples was carried out using a Rigaku powder diffractometer at ambient temperature in the angle range of 5–30°. The crystalline sample was obtained by recrystallization of **1PH** from EtOH/acetone while the SmE phases were prepared by heating samples on glass slides to the isotropic phase (~230°C) and cooling. The unit cell parameters were calculated and the diffraction patterns simulated using the JADE 3.0 software package.

5.2. *4-Octyloxy-4′-(12-pentyl-1,12-dicarbado-decaboran-1-yl)biphenyl (**1BC**)*

A mixture of bromide **2BC** [8] (0.20 g, 0.54 mmol), 4-octyloxybenzeneboronic acid ester (**3**) [7] (0.17 g, 0.62 mmol), benzene (4 ml), 2M Na_2CO_3 (2 ml), and tetrakis(triphenylphosphine)palladium (0.013 g) was stirred and heated under reflux in a nitrogen atmosphere until it become a grey-black suspension of reduced Pd and GC showed no more starting bromide **2BC** (about 2 days). The mixture was diluted with water and hexane, the organic layer was separated, dried (Na_2SO_4), and passed through a silica gel plug. The plug was washed with hexane (25 ml) and the colourless eluent was concentrated in vacuum leaving 170 mg of white solid crude product. Impurities (11 mg) were removed by vacuum sublimation (up to 160°C/0.1 mm Hg) and the remaining product was recrystallized twice from pentane (0°C) to give 135 mg product (50% yield): m.p. 71.7°C; ^{1}H NMR δ 0.8–3.5 (br m, 10H), 0.82 (t, $J = 7.2$ Hz, 3H), 0.86 (t, $J = 6.0$ Hz, 3H), 1.10–1.52 (m, 16H), 1.60–1.66 (m, 2H), 1.71–1.81 (m, 2H), 3.95 (t, $J = 6.5$ Hz, 2H), 6.90 (d, $J = 8.5$ Hz, 2H), 7.20 (d, $J = 8.3$ Hz, 2H), 7.31 (d, $J = 8.2$ Hz, 2H), 7.40 (d, $J = 8.5$ Hz, 2H); ^{13}C NMR (C_6D_6) δ 14.03, 14.34, 22.47, 23.05, 26.43, 29.57, 29.66, 29.75, 31.38, 32.19, 38.20, 68.01, 81.67, 115.16, 126.62, 127.95, 128.31, 132.57, 134.96, 141.34, 159.59; ^{11}B NMR δ − 13.5 ($J_{BH} = 167$ Hz); IR 2926, 2855, 2609, 1607, 1499, 1466, 1247, 817 cm^{-1}; EIMS, EIMS, m/e: 497–493 (max at 495, M, 88) 384–380 (max at 382, 100). Elemental anal: calcd for $C_{27}H_{46}B_{10}O$, C 65.55, H 9.37; found C 65.53, H 9.44%.

5.3. *4-Octyloxy-4′-(4-trans-pentylcyclohexyl)biphenyl (**1CH**)*

A filtered solution of 4-octyloxyphenylmagnesium bromide (**4**), obtained from 4-octyloxybromobenzene (5.0 g, 17.5 mmol) and magnesium (0.5 g, 20 mmol) in THF (20 ml), was added dropwise (15 min) to a stirred dispersion of anhydrous $NiBr_2$ (50 mg) and 1-iodo-4-(*trans*-4-pentylcyclohexyl)benzene [10] (5.0 g, 14.5 mmol) in anhydrous THF (20 ml) at 40–50°C. The resulting dark brown solution was stirred at 40–50°C for 4 h and left overnight at room temperature. The reaction mixture was poured into diluted (1 : 10) hydrochloric acid (150 ml) and extracted with benzene. The organic layer was washed with diluted (1 : 10) hydrochloric acid (2 × 20 ml), water (3 × 20 ml), and brine, dryed ($MgSO_4$) and evaporated. The crude product was recrystallized several times from an ethanol–acetone mixture (3 : 1 vol.) to give 2.1 g (33% yield) of product: m.p. 56.0°C; ^1H NMR δ 0.88 (t, $J = 6.7$ Hz, 3H), 0.89 (t, $J = 6.7$ Hz, 3H), 0.95–1.10 (m, 2H), 1.15–1.50 (m, 20H), 1.72–1.93 (m, 7H), 2.48 (tt, $J_1 = 12.1$ Hz, $J_2 = 3.0$ Hz, 1H), 3.97 (t, $J = 6.6$ Hz, 2H), 6.92 (d, $J = 8.7$ Hz, 2H), 7.23 (d, $J = 8.2$ Hz, 2H), 7.44 (d, $J = 8.1$ Hz, 2H), 7.47 (d, $J = 8.7$ Hz, 2H); ^{13}C NMR δ 14.12, 22.66, 22.72, 26.06, 26.66, 29.25, 29.30, 29.37, 31.82, 32.21, 33.61, 34.35, 37.30, 37.39, 44.23, 68.04, 114.65, 126.56, 127.17, 127.92, 133.49, 138.40, 146.32, 158.46; IR 2955, 2921, 2854, 1466, 1448, 1117, 820 cm^{-1}; EIMS, *m/e*: 435 (33, M + 1), 434 (100, M), 322 (25), 209 (25), 196 (27). Elemental anal: calcd for $C_{31}H_{46}O$, C 85.65, H 10.67; found C 85.75, H 10.73%.

5.4. *4-Octyloxy-4′-(4-pentylbicyclo[2.2.2]octan-1-yl)-biphenyl (**1BO**)*

This compound was obtained from 1-iodo-4-(4-pentylbicyclo[2.2.2]oct-1-yl)benzene [10] as described for **1CH**: m.p. 96.7°C; ^1H NMR δ 0.89 (t, $J = 6.9$ Hz, 6H), 1.08–1.39 (m, 16H), 1.42–1.52 (m, 8H), 1.75–1.86 (m, 8H), 3.98 (t, $J = 6.6$ Hz, 2H), 6.94 (d, $J = 8.7$ Hz, 2H), 7.36 (d, $J = 8.5$ Hz, 2H), 7.47 (d, $J = 8.2$ Hz, 2H), 7.49 (d, $J = 8.7$ Hz, 2H); ^{13}C NMR δ 14.11, 22.66, 22.73, 23.41, 26.07, 29.25, 29.30, 29.37, 30.74, 31.55, 31.82, 32.68, 32.89, 34.66, 41.71, 68.04, 114.65, 125.94, 126.25, 127.91, 133.38, 137.91, 148.80, 158.46; IR 2935, 2923, 2856, 1604, 1466, 1455, 1245, 813 cm^{-1}; EIMS, *m/e*: 461 (38, M + 1), 460 (100, M), 334 (16), 222 (24). Elemental anal: calcd for $C_{33}H_{48}O$, C 86.03, H 10.50; found C 86.10, H 10.52%.

5.5. *4-Octyloxy-4″-pentylterphenyl (**1PH**)*

This compound was obtained from 4-iodo-4′-pentylbiphenyl as described for **1CH** [11]: m.p. 96.7°C; ^1H NMR δ 0.89 (t, $J = 6.8$ Hz, 3H), 0.91 (t, $J = 6.7$ Hz, 3H), 1.26–1.40 (m, 12H), 1.42–1.53 (m, 2H), 1.61–1.71 (m, 2H), 1.76–1.86 (m, 2H), 2.65 (t, $J = 7.7$ Hz, 2H), 4.00 (t, $J = 6.5$ Hz, 2H), 6.98 (d, $J = 8.7$ Hz, 2H), 7.27 (d, $J \sim 8.5$ Hz (partial overlap with solvent), 2H), 7.55 (d, $J = 8.2$ Hz, 2H), 7.56 (d, $J = 8.7$ Hz, 2H), 7.61 (d, $J = 8.8$ Hz, 2H), 7.63 (d, $J = 8.8$ Hz, 2H); ^{13}C NMR δ 14.05, 14.11, 22.57, 22.66, 26.07, 29.26, 29.30, 29.38, 31.19, 31.57, 31.82, 35.59, 68.08, 114.79, 126.78, 126.93, 127.23, 127.94, 128.83, 133.01, 138.06, 139.36, 139.45, 142.07, 158.74; IR 2953, 2922, 2853, 1606, 1492, 1466, 1400, 1286, 1260, 805 cm^{-1}; EIMS, *m/e*: 429 (35, M + 1), 428 (100, M), 316 (26), 259 (58). Elemental anal: calcd for $C_{31}H_{40}O$, C 86.86, H 9.41; found C 86.86, H 9.39%.

This project has been funded in part by the National Research Council under the Collaboration in Basic Science and Engineering Program. Support for this project has also been provided by the NSF CAREER grant (DMR-9703002). We are grateful to Ms Michelle Mierzwa for her technical assistance with chemical analysis, Dr John Desper for making his Rigaku X-ray diffractometer available to us, and Prof. Jan Przedmojski for helpful comments.

References

[1] Kaszynski, P., Huang, J., Jenkins, G. S., Bairamov, K. A., and Lipiak, D., 1995, *Mol. Cryst. liq. Cryst.*, **260**, 315.

[2] Kaszynski, P., and Lipiak, D., 1995, in *Materials for Optical Limiting*, edited by R. Crane, K. Lewis, E. V. Stryland and M. Khoshnevisan (MRS), Vol. 374, p. 341.

[3] Kaszynski, P., Lipiak, D., Bairamov, K. A., Brady, E., Patel, M. K., and Laska, J., 1997, in *Advances in Boron Chemistry*, edited by W. Siebert (The Royal Society of Chemistry), p. 507.

[4] Douglass, A. G., Mierzwa, M., and Kaszynski, P., 1998, *SPIE*, **3319**, 59.

[5] Czuprynski, K., and Kaszynski, P., *Liq. Cryst.* (submitted).

[6] Douglass, A. G., Czuprynski, K., Mierzwa, M., and Kaszynski, P., 1998, *J. Mater. Chem.*, **10**, 2399; 1998, *Chem. Mater.*, **8**, 2391.

[7] Gray, G. W., Hird, M., and Toyne, K., 1991, *Mol. Cryst. liq. Cryst.*, **195**, 221.

[8] Douglass, A. G., Mierzwa, M., and Kaszynski, P., unpublished results.

[9] Miyaura, N., Yanagi, T., and Suzuki, A., 1981, *Synth. Commun.*, **11**, 513.

[10] Adamska, G., Dabrowski, R., Dziaduszek, J., Kenig, K., and Zytynski, E., 1978, *Biul. WAT*, **11**, 91.

[11] Dabrowski, R., Witkiewicz, Z., and Kenig, K., 1980, *Mol. Cryst. liq. Cryst.*, **58**, 251.

[12] Ikoma, Y., Taya, F., Ozaki, E., Higuchi, S., Naoi, Y., and Fuji-i, K., 1990, *Synthesis*, 147.

[13] Toyne, K., 1987, in *Thermotropic Liquid Crystals*, edited by G. W. Gray (John Wiley and Sons), p. 42.

[14] McMillan, W. L., 1971, *Phys. Rev. A*, **4**, 1238.

[15] Gray, G. W., and Goodby, J. W. G., 1984, *Smectic Liquid Crystals* (Leonard Hill), p. 93.
[16] Bondi, A., 1964, *J. phys. Chem.*, **68,** 441.
[17] Demus, D., Fietkau, C., Schubert, R., and Kehlen, H., 1974, *Mol. Cryst. liq. Cryst.*, **25,** 215.
[18] Czuprynski, K., 1990, *Mol. Cryst. liq. Cryst.*, **192,** 47.
[19] Cladis, P. E., 1981, *Mol. Cryst. liq. Cryst.*, **67,** 177.
[20] Dabrowski, R., and Czuprynski, K., 1988, *Cryst. Res. Technol.*, **23,** 1545.
[21] Domon, M., and Billard, J., 1979, *J. Phys. (Paris)*, **40,** C3-413.
[22] Fukui, M., and Matsunaga, Y., 1981, *Bull. chem. Soc. Japan*, **54,** 3137.
[23] Araya, K., and Matsunaga, Y., 1981, *Mol. Cryst. liq. Cryst.*, **67,** 153.
[24] Modhusudana, N. V., 1990, in *Liquid Crystals Applications and Uses*, edited by B. Bahaddur (Utopia Press), Vol. 1, pp. 37-90.
[25] Gaussian 94, Revision E.1, [Frisch, M. J., Trucks, G. W., Schlegel, H. B., Gill, P. M., Johnson, B. G., Robb, M. A., Cheeseman, J. R., Keith, T., Petersson, G. A., Montgomery, J. A., Raghavachari, K., Al-Laham, M. A., Zakrzewski, V. G., Ortiz, J. V., Foresman, J. B., Cioslowski, J., Stefanov, B. B., Nanayakkara, A., Challacombe, M., Peng, C. Y., Ayala, P. Y., Chen, W., Wong, M. W., Andres, J. L., Replogle, E. S., Gomperts, R., Martin, R. L., Fox, D. J, Binkley, J. S., Defrees, D. J., Baker, J., Stewart, J. P., Head-Gordon, M., Gonzalez, C., and Pople, J. A.] Gaussian, Inc., Pittsburgh PA, 1995.